

See discussions, stats, and author profiles for this publication at: <https://www.researchgate.net/publication/229927242>

# The heterogeneous reaction of HONO and HBr on ice and on sulfuric acid

ARTICLE *in* BERICHTE DER BUNSENGESELLSCHAFT/PHYSICAL CHEMISTRY CHEMICAL PHYSICS · JUNE 1997

DOI: 10.1002/bbpc.19971010609

---

CITATIONS

13

---

READS

31

## 2 AUTHORS:



Sabine Seisel

Ruhr-Universität Bochum

22 PUBLICATIONS 273 CITATIONS

SEE PROFILE



Michel J Rossi

Paul Scherrer Institut

259 PUBLICATIONS 6,468 CITATIONS

SEE PROFILE

# The Heterogeneous Reaction of HONO and HBr on Ice and on Sulfuric Acid

Sabine Seisel and Michel J. Rossi\*)

Laboratoire de Pollution Atmosphérique et Sol (LPAS), Swiss Federal Institute of Technology (EPFL), CH-1015 Lausanne, Switzerland

**Key Words:** Adsorption / Chemical Kinetics / Heterogeneous Reactions / Interfaces / Surfaces

The heterogeneous reactions of HONO with HBr on ice, solid and supercooled liquid  $\text{H}_2\text{SO}_4$  solution (40–95 wt%) were studied in the temperature range 180 to 200 K for the solid substrates (ice,  $\text{H}_2\text{SO}_4$ ) and 210 to 270 K for the liquid solutions of  $\text{H}_2\text{SO}_4$  using a Knudsen flow reactor.

The uptake coefficient of HONO onto frozen aqueous HBr solutions at 190 K was determined and resulted in a mean value of  $\gamma = (2.3 \pm 1.2) \cdot 10^{-2}$ . On ice the HBr uptake rate is high with a mean value of  $\gamma = 0.32 \pm 0.12$  between 180 and 200 K and is unaffected by the presence of HONO. The uptake of HONO onto ice is a function of the HBr concentration in the condensed phase and for the highest HBr flows used an uptake coefficient of  $\gamma = 2.2 \cdot 10^{-2}$  was found.

On frozen  $\text{H}_2\text{SO}_4$  solutions the uptake coefficient of HBr varies with the concentration of the solution from about 0.25 at 10 wt% to less than  $1 \cdot 10^{-4}$  in the absence and  $5 \cdot 10^{-4}$  in the presence of HONO at 95 wt%. The uptake of HONO in the presence of HBr was found to vary with the HBr concentration and to be approximately a factor of two lower than on the ice surface.

On liquid  $\text{H}_2\text{SO}_4$  the uptake coefficients of HBr and HONO both strongly depended on the concentration of the solution. HONO shows the greatest interaction at 95 wt% with  $\gamma = 2 \cdot 10^{-2}$  and decreases to about  $5 \cdot 10^{-3}$  at 40 wt%. In comparison HBr only shows a weak interaction of  $\gamma$  of approximately  $5 \cdot 10^{-4}$  at 95 wt% and a strong interaction of  $\gamma = 4 \cdot 10^{-2}$  at 40 wt%.

On all three substrates the concurrent uptake of HONO and HBr was found to be reactive forming the only identified bromine containing reaction product  $\text{BrNO}$ . The variation of the substrates from strong acid liquid to solid neutral provides information about the nature of the heterogeneous interaction.

## 1. Introduction

The atmospheric trace gas nitrous acid plays an important role in the tropospheric daytime chemistry due to its rapid photolysis to OH and NO. During the nighttime HONO accumulates and reaches levels of up to 8 ppb just before sunrise [1–4]. The formation processes of HONO are not yet completely understood and heterogeneous reactions of NO,  $\text{NO}_2$  and  $\text{H}_2\text{O}$  are assumed to be the most probable [1, 5]. At sunrise HONO undergoes rapid photolysis and the formed hydroxyl radicals initiate the diurnal oxidative cycles [6, 7]. Furthermore, together with other pollutants ( $\text{NO}_x$ ,  $\text{SO}_2$ ) and aerosols HONO is directly emitted into the upper troposphere by aircraft [8, 9]. The influence of these exhausts on the atmosphere is complex and not well known [9].

Heterogeneous reactions of HONO during the daytime are not very likely because of rapid photolysis. However, during the nighttime heterogeneous conversion of HONO may take place in the presence of particulate matter and/or aerosols. Recently the heterogeneous reaction of HONO with HCl was studied on sulfuric acid and on ice [10, 11]. The authors found that HCl is converted to ClNO on both substrates. ClNO photolyses rapidly [12] and therefore provides a source of activated chlorine, which may affect the gas phase chemistry of the atmosphere.

Heterogeneous activation of HBr is thought to play a minor role due to its small concentration in the atmosphere [13]. Only a few studies on the heterogeneous reaction of HBr exist [14–18]. The general finding is that HBr reacts more efficiently than the analogous HCl on ice and on sulfuric acid which may compensate somewhat for the low

abundance. Nevertheless, HBr may accumulate on ice or in sulfuric acid aerosols in cases where high particle densities occur e.g. in clouds or contrails. Thus heterogeneous reactions of HBr may contribute to the halogen activation in the upper troposphere and lower stratosphere.

In this work we present the results of our experiments on the heterogeneous reaction of HONO with HBr. In analogy to the investigations of the reaction of HONO with HCl we studied the reaction on ice and supercooled sulfuric acid solutions of various concentration. In order to assess the role of the surface further experiments have been conducted on frozen sulfuric acid at different concentrations as a link between a solid neutral (ice) and an acidic liquid ( $\text{H}_2\text{SO}_4$ ) surface.

## 2. Experimental Setup

The experiments were performed in a Teflon-coated Knudsen flow reactor operating in the molecular flow regime. The experiment will only briefly be presented here as details are discussed elsewhere [19–21]. The apparatus is divided into three main parts: a gas handling system, the Knudsen reactor which may be combined with different sample supports, and a vacuum chamber housing the differentially pumped mass spectrometer (MS) (Fig. 1). As a sample support we use a low temperature cell in which the sample can be cooled down to 150 K. A programmable temperature controller maintained the final temperature to  $\pm 0.5$  K at an accuracy of  $\pm 2$  K. A detailed description of the support is given elsewhere [21].

The gases under study were introduced into the Knudsen reactor from the gas handling system by either using a capillary for pressure reduction or a pulsed valve. The gases leave the Knudsen reactor through an escape orifice whose

\*) Author to whom correspondence should be addressed.

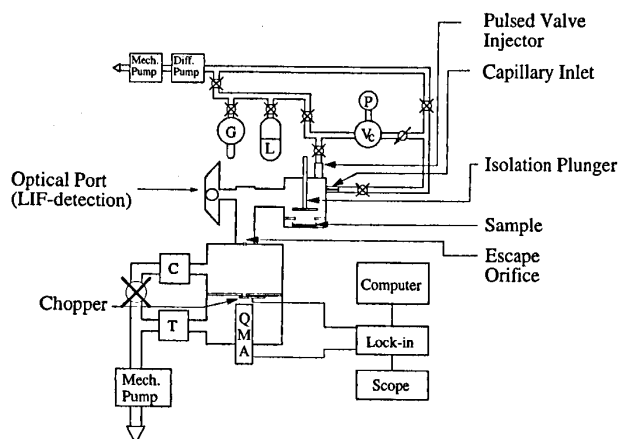


Fig. 1

Scheme of the experimental setup. The upper part represents the gas-handling system, including a reservoir for the gaseous reactant (G and L), a calibrated volume (Vc), and a pressure gauge (P) for gas-flow calibrations. The Knudsen cell is mounted on a differentially pumped vacuum chamber, evacuated by cryogenic (C) and a turbomolecular pump (T). The flux of gaseous species is measured by a mass spectrometer (QMA) located in the lower of the two vacuum chambers

diameter (1, 4, 8, 15 mm) determines the residence time of the molecules in the Knudsen reactor. The rate constant for the effusive loss  $k_{\text{esc}}$  is given by the kinetic theory of gases and was measured routinely for each compound. By entering the differentially pumped vacuum chamber the molecules form an effusive beam. After modulation by a chopper operating at 160 Hz at the entrance of the lower stage the beam is detected by a quadrupole mass spectrometer (MS).

In a steady state experiment the concentration of the reactant gas is monitored while bypassing the reactive surface. Lifting the plunger (Fig. 1) causes a change in the steady state signal if the gas interacts with the surface on the time scale of the experiment. As long as the uptake is first order in the gas density, the difference of the two steady state concentrations yields the rate constant for the uptake,  $k_{\text{uni}}$ , according to the relation:

$$k_{\text{uni}} = \left( \frac{S_i}{S_f} - 1 \right) \cdot k_{\text{esc}}$$

where  $S_i$  and  $S_f$  are the steady state MS signals before and during reaction, respectively, and  $k_{\text{esc}}$  is the rate constant for the effusive loss. Dividing the rate constant  $k_{\text{uni}}$  by the collision frequency with the reactive surface  $A_S$  the dimensionless uptake coefficient  $\gamma$  is obtained.

Pulsed valve experiments were performed by introducing a short pulse of gaseous HONO (typically 1 ms) into the Knudsen reactor and monitoring the escape rate of the gas molecules out of the Knudsen chamber in real time using MS detection. In the reference experiment the reactive surface was isolated and the observed signal corresponded to an exponential decay according to its rate constant for effusive loss,  $k_{\text{esc}}$ . In the following experiment the sample

was exposed to an identical pulse of gas molecules, and in the case of an interaction the observed decay constant represents the sum of the effusive and the reactive loss:  $k_{\text{decay}} = k_{\text{uni}} + k_{\text{esc}}$ . The parameters characterizing the Knudsen cell used in this study are listed in Table 1.

Table 1  
Knudsen cell parameters

Reactor parameter	Value
Volume	2000 cm <sup>3</sup>
Gas number density	(1–1000) · 10 <sup>10</sup> cm <sup>-3</sup>
Sample area	15.3 cm <sup>2</sup>
Sample collision frequency ( $\omega$ )	$27.8 \left( \frac{T}{M} \right)^{0.5} \text{ s}^{-1}$
Orifice diameter	1, 4, 8 and 15 mm
Escape rate constant ( $\varnothing = 1 \text{ mm}$ ) ( $k_{\text{esc}}$ )	$1.6 \cdot 10^{-2} \left( \frac{T}{M} \right)^{0.5} \text{ s}^{-1}$
Escape rate constant ( $\varnothing = 4 \text{ mm}$ ) ( $k_{\text{esc}}$ )	$0.2 \left( \frac{T}{M} \right)^{0.5} \text{ s}^{-1}$
Escape rate constant ( $\varnothing = 8 \text{ mm}$ ) ( $k_{\text{esc}}$ )	$0.8 \left( \frac{T}{M} \right)^{0.5} \text{ s}^{-1}$
Escape rate constant ( $\varnothing = 15 \text{ mm}$ ) ( $k_{\text{esc}}$ )	$2.1 \left( \frac{T}{M} \right)^{0.5} \text{ s}^{-1}$

The gas densities were determined in mass-flow calibrations. The flow rate into the Knudsen reactor was measured by recording the pressure change in a closed calibrated volume behind the capillary while monitoring the corresponding MS signal. The flow of molecules into the cell may then be related to the density of the gas molecules in the cell. Typical flow rates for HBr were  $2 \cdot 10^{14}$  to  $6 \cdot 10^{15}$  mol/s corresponding to densities of  $2 \cdot 10^{11}$  to  $8 \cdot 10^{12}$  mol/cm<sup>3</sup> while the HONO flow was approximately  $1 \cdot 10^{15}$  to  $1 \cdot 10^{16}$  mol/s corresponding to a density of  $1 \cdot 10^{11}$  to  $1 \cdot 10^{13}$  mol/cm<sup>3</sup>. The mass spectrometer settings were chosen to yield a sensitivity of approximately  $10^{10}$  to  $10^{11}$  mol/cm<sup>3</sup> at a signal to noise ratio greater than 2. The sulfuric acid solutions were prepared by diluting 95 wt% H<sub>2</sub>SO<sub>4</sub> with demineralized water. The concentrations of the resulting solutions were 10, 40, 52, 60, 69 and 80 wt% H<sub>2</sub>SO<sub>4</sub> with an accuracy of 2% and were checked by acid base titration. The aqueous HBr solutions were prepared in the same way. By diluting a stock solution of 50 wt% HBr concentrations of 0.08, 0.8, 8, 20, 29 and 40 wt% with an accuracy of 5% were obtained. For preparing the cold sample surfaces approximately 5 ml of the respective liquid were poured into the sample support at ambient temperature. After mounting the support on the Knudsen reactor the sample was cooled down to the desired temperature in about 15 min and subsequently evacuated. We checked the state of the sample, whether supercooled liquid or frozen solid, by comparing the measured water vapor pressure

with the equilibrium water vapor pressure given in the literature. The solidification of the liquids could be visually checked. However, we may not exclude that in certain cases a thin liquid layer remains above the solid. On the basis of their visual appearance we have classified the surfaces into solids and liquids. Nearly all reactive surfaces used in this study contain a certain amount of water. By lifting the plunger a sudden pressure increase due to evaporating water in the reactor may occur thus briefly perturbing the mass spectrometric detection. To avoid this a constant external water flow corresponding to the water vapor pressure of the sample was supplied to the Knudsen reactor. When the external water flow corresponded to the equilibrium vapor pressure of the cold sample no net uptake of water vapor could be observed upon opening and closing the sample compartment. In addition, we compared the amount of the external water flow with the water vapor pressure given in the corresponding phase diagram.

Gaseous HBr was commercially available and was purified by distillation until no more molecular bromine could be detected by MS. HONO was prepared according to the procedure of Fenter and Rossi [11] by adding 5 to 8 drops of 50 wt%  $\text{H}_2\text{SO}_4$  to 50 ml of a stirred aqueous  $\text{NaNO}_2$  solution at 273 K. The gases produced from the source were NO as main product,  $\text{NO}_2$  and HONO. The quantity of  $\text{NO}_2$  and HONO emanating from the source was approximately 50 and 10% that of NO, respectively (for more details see Ref. [11]).  $\text{BrNO}$  was synthesized by adding  $\text{Br}_2$  to an excess of NO followed by distillation at 200 K. A mass spectrum of the resulting product showed only the fragments of  $\text{BrNO}$  ( $\text{BrNO}^+$ ,  $\text{BrN}^+$ ,  $\text{Br}^+$  and  $\text{NO}^+$ ), and no  $\text{Br}_2$  was detected. The mass spectra of the compounds used in this study are listed in Table 2.

Table 2  
Mass spectral data

Species	Parent peak <sup>a)</sup>	Fragment <sup>a)</sup>	Fragment <sup>a)</sup>	Fragment <sup>a)</sup>
$\text{BrNO}$	109, 111 (1.2)	93, 95 (1.2)	79, 81 (9)	30 (100)
HONO	47 (14)	30 (100)		
HBr	80, 82 (100)	79, 81 (40)		
$\text{Br}_2$	160 (100)	79, 81 (20)		

<sup>a)</sup> Ion mass with peak intensity in parentheses, given as percent of the most intense peak. The numbers in italics indicate the mass fragments which were used to monitor the species by MS

### 3. Experimental Results

#### 3.1 Uptake of HBr

The HBr uptake onto ice is fast and does not saturate over the duration of the experiment (up to 10 min). A mean value for the uptake coefficient of  $\gamma = 0.32 \pm 0.12$  has been determined where the uncertainty represents one standard deviation. In the range of 180 to 200 K a slight negative temperature dependence was observed (Fig. 2). No dependence of the uptake coefficient on the HBr concentration could be

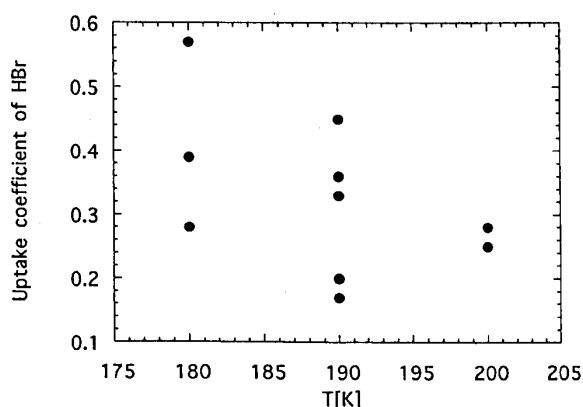


Fig. 2  
Uptake coefficient of HBr on ice as a function of temperature. Experimental conditions are summarized in Table 3

detected by varying the HBr flow approximately by a factor of 50 which clearly indicates that the uptake of HBr onto the ice surface is first order with respect to HBr. This is further confirmed by using different escape orifices which led to the same value for the reactive loss,  $k_{\text{uni}}$ .

The uptake of HBr on frozen  $\text{H}_2\text{SO}_4$  solutions changes slightly with the  $\text{H}_2\text{SO}_4$  concentration. All experiments were performed at 190 K with a balancing water flow. The crystallization of the  $\text{H}_2\text{SO}_4$  solution was visually checked. However, we are not able to assess whether the solid consists of only one or more phases, e.g. of ice and sulfuric acid hydrate. The highest uptake coefficient of  $\gamma = 0.25$  was observed at 10 wt%  $\text{H}_2\text{SO}_4$  approaching the one for ice. With increasing  $\text{H}_2\text{SO}_4$  concentration the uptake of HBr decreases reaching  $\gamma = 0.18$  at 60 wt%  $\text{H}_2\text{SO}_4$ . At 95 wt%  $\text{H}_2\text{SO}_4$  the amount of HBr taken up is below the detection limit of the mass spectrometer, that is HBr taken up is less than 5% of the initial concentration at a residence time of 3 s in the Knudsen reactor (Table 1).

The interaction of HBr with liquid supercooled  $\text{H}_2\text{SO}_4$  shows a similar trend as with solid  $\text{H}_2\text{SO}_4$  except for an uptake coefficient lower by a factor of 10:  $\gamma = 0.05$  at 40 wt%  $\text{H}_2\text{SO}_4$ ,  $\gamma = 0.01$  at 52 wt%  $\text{H}_2\text{SO}_4$  and  $5 \cdot 10^{-4}$  at 69 wt%. The experimental results are presented in Table 3.

#### 3.2 Reaction of HONO and HBr on Solid Surfaces

##### 3.2.1 HONO on Frozen HBr Solutions

HONO is readily taken up by frozen aqueous HBr solutions. In Fig. 3 the steady state MS signal of HONO ( $m/e = 47$ ) is shown before, during and after the exposure to a 8 wt% HBr solution at 190 K. By lifting the plunger we observe a drop in the HONO signal indicating an interaction of HONO with the surface. During the reaction increases in the MS signals  $m/e$  79/81, 93/95 and 109/111 were observed which were unambiguously assigned to  $\text{BrNO}$ . The observed intensity ratio was found to be in agreement with the mass spectrum of pure  $\text{BrNO}$ . No change in the MS signals at  $m/e$  80 (HBr) and 160 ( $\text{Br}_2$ ) could be detected. By

Table 3

Experimental results for the uptake of HBr. The average value for the uptake of HBr on ice is  $\gamma = 0.32 \pm 0.12$  (the uncertainty represents  $1\sigma$ )

Sample	<i>T</i> [K]	<i>F</i> <sup>a</sup> (HBr) <sup>a</sup> [mol/s]	$\gamma$	Orifice <sup>b</sup>
Ice	180	2.35(15)	0.39	8
Ice	180	2.95(15)	0.28	8
Ice	180	2.56(15)	0.57	4
Ice	190	2.67(14)	0.45	4
Ice	190	3.68(15)	0.20	8
Ice	190	2.10(15)	0.33	8
Ice	190	3.17(14)	0.17	4
Ice	190	3.16(14)	0.36	4
Ice	200	2.64(15)	0.25	8
Ice	200	1.69(15)	0.28	4
Ice	200	2.18(15)	0.25	4
10 wt% H <sub>2</sub> SO <sub>4</sub> (s)	190	1.83(15)	0.25	4
40 wt% H <sub>2</sub> SO <sub>4</sub> (s)	190	2.57(15)	0.21	4
40 wt% H <sub>2</sub> SO <sub>4</sub> (s)	190	2.83(15)	0.19	4
40 wt% H <sub>2</sub> SO <sub>4</sub> (s)	190	2.60(15)	0.28	8
40 wt% H <sub>2</sub> SO <sub>4</sub> (l)	210	3.12(15)	0.049	4
52 wt% H <sub>2</sub> SO <sub>4</sub> (s)	190	2.62(15)	0.20	4
52 wt% H <sub>2</sub> SO <sub>4</sub> (s)	190	2.41(15)	0.23	4
52 wt% H <sub>2</sub> SO <sub>4</sub> (s)	190	2.41(15)	0.21	8
52 wt% H <sub>2</sub> SO <sub>4</sub> (l)	210	2.72(15)	0.012	4
60 wt% H <sub>2</sub> SO <sub>4</sub> (s)	190	2.62(15)	0.18	4
69 wt% H <sub>2</sub> SO <sub>4</sub> (l)	220	2.78(15)	5 (-4)	4
95 wt% H <sub>2</sub> SO <sub>4</sub> (s)	220	2.60(15)	<1 (-4)	4

<sup>a</sup>) Flow into the Knudsen cell

<sup>b</sup>) Diameter in mm of the orifice, (s) solid, (l) liquid

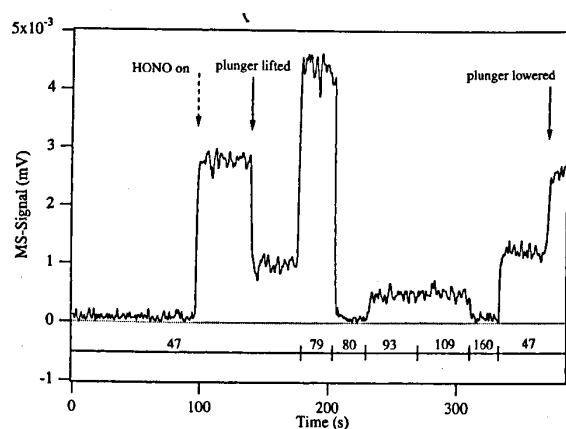


Fig. 3

Steady state experiment of HONO on a 8 wt% frozen HBr solution at 190 K and 4 mm escape orifice. The numbers at the bottom indicate the quadrupole mass filter setting. At 150 s the plunger is lifted and the sample is exposed to a flow of HONO ( $F = 2.59 \cdot 10^{15}$  mol/s). Rapid uptake is observed accompanied by the production of BrNO ( $m/e$  79, 93, 109) at 100% yield

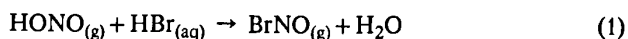
lowering the plunger, thus isolating the substrate from the flow of HONO, the initial signal intensity for HONO reappeared. Since HBr was not found to evaporate from the substrate the observed loss of HONO is only due to the interaction with the reactive surface. The uptake of HONO was measured on HBr solutions of 0.08, 0.8, 8, 20, 29, 42 and 50 wt% HBr at 190 K. Except for the 42 wt% one all solutions were frozen as a white ice like solid which was

visually checked. The 42 wt% HBr solution had the appearance of a viscous liquid. According to the melting diagram the HBr-H<sub>2</sub>O system [22, 23] has an eutectic point at 184 K and 39.4 wt% HBr which is close to 42 wt%. Therefore, lower temperatures are required to crystallize the substrate in this concentration range.

No saturation of the HONO uptake for HBr concentrations below 20 wt% were observed. But for HBr concentrations higher than 20 wt% the rate of HONO uptake decreases with time. For the 40 and 50 wt% HBr solutions complete saturation of the HONO uptake was observed within 1 to 2 min. During these experiments the initial HONO flow was held nearly constant at approximately  $2 \cdot 10^{15}$  mol/s. The initial uptake coefficient of HONO showed no dependence on the concentration of a given HBr solution and was determined to be  $\gamma = (2.3 \pm 1.2) \cdot 10^{-2}$  (the uncertainty represents one standard deviation). According to the melting diagram [22, 23] the cooling of a HBr solution lower than 39.4 wt% in HBr results in the formation of ice and a more highly concentrated HBr solution. At 190 K the liquid should always have a HBr concentration close to the eutectic point (39.4 wt%) regardless of its initial value. We can therefore not exclude the formation of a thin liquid layer above the ice. The measured uptake coefficients may therefore correspond to the uptake of HONO on a liquid HBr solution of about 40 wt% assuming equilibrium between ice and the liquid.

On a 8 wt% HBr solution additional experiments were performed by using the pulsed valve as a gas inlet for HONO. The analysis showed that HONO was taken up with a rate constant  $k_{\text{uni}}$  of  $1.15 \text{ s}^{-1}$  which corresponds to  $\gamma = 1.5 \cdot 10^{-2}$ . This value agrees well with the results of the steady state experiments and indicates that no saturation of the surface has occurred on the time scale of the experiment. Identical decay rate constants were determined for the MS signals at  $m/e = 79$  and 109 confirming that the masses belong to the same parent. Experimental results are given in Table 4.

These experiments confirm that the only bromine containing product of the reaction of HONO with HBr is BrNO. Br<sub>2</sub> and HBr were not observed. BrNO<sub>2</sub> which also contributes to  $m/e$  79 and 93 may be excluded since the observed intensity ratio 79/93/109 corresponds to pure BrNO. In addition, no difference in the escape rate constants for masses 79 and 109 was found pointing to the same parent molecule. The evaluation of the mass balance resulted in a  $100 \pm 15\%$  yield of BrNO with respect to the amount of HONO taken up at excess HBr on the substrate indicating that BrNO is nonreactive on these substrates. Therefore the heterogeneous reaction may be written as follows:



### 3.2.2 Reaction of HONO and HBr on Ice

HONO is taken up on an ice surface with an initial uptake coefficient of about  $1 \cdot 10^{-3}$  and saturation takes place in a few seconds [11]. However, in the presence of gas phase

Table 4

Experimental results for the uptake of HONO on frozen HBr solutions at  $T = 190$  K. The average value of  $\gamma$  is  $(2.3 \pm 1.2) \cdot 10^{-2}$  (the uncertainty represents  $1\sigma$ )

HBr [wt%]	$F^i$ (HONO) <sup>a)</sup> [mol/s]	$F^R$ (HONO) <sup>b)</sup> [mol/s]	$F^R$ (BrNO) <sup>c)</sup> [mol/s]	$\gamma$	Orifice <sup>d)</sup>
50	1.54(15)	8.43(14)	8.70(14)	0.041	15
40	1.33(15)	1.43(14)	5.50(13)	0.014	15
40	9.38(14)	1.06(14)	1.15(14)	0.015	15
40	2.21(15)	8.89(14)		0.022	8
30	1.71(15)	1.42(15)		0.035	4
20	3.00(15)	2.37(15)	2.15(15)	0.034	4
20	1.98(15)	5.57(14)	3.78(14)	0.013	8
20	3.64(15)	2.57(15)	2.44(15)	0.010	1
8	1.68(15)	1.42(15)	1.34(15)	0.043	4
8	2.73(15)	1.79(15)	2.00(15)	0.016	4
8	1.56(15)	1.27(15)	1.29(15)	0.040	4
8	1.81(15)	1.49(15)	1.46(15)	0.040	4
8	pv <sup>e)</sup>			0.015	4
0.8	1.57(15)	1.01(14)	1.08(15)	0.015	4
0.8	1.29(15)	8.16(14)	8.56(14)	0.014	4
0.08	1.05(15)	6.87(14)	1.04(15)	0.015	4
0.08	8.91(14)	2.92(14)	4.20(14)	0.016	8

<sup>a)</sup> Flow into the Knudsen cell

<sup>b)</sup> Flow to the surface defined by  $F^{\text{in}} - F^{\text{out}}$

<sup>c)</sup> Flow from the surface

<sup>d)</sup> Diameter in mm of orifice

<sup>e)</sup> Pulsed valve experiment

HBr the uptake of HONO is enhanced by up to a factor of twenty and does not saturate. A typical result at 190 K is shown in Fig. 4. By lifting the plunger a sudden drop in the HONO signal at  $m/e$  47 is observed followed by saturation due to physical uptake onto the ice surface [11]. At 60 s the HBr flow is turned on resulting in a decrease of the HONO partial pressure (upper trace) and the appearance of BrNO ( $m/e$  109, lower trace) on the time scale of a few seconds. The uptake of HBr ( $m/e$  80, middle trace) is identical to the

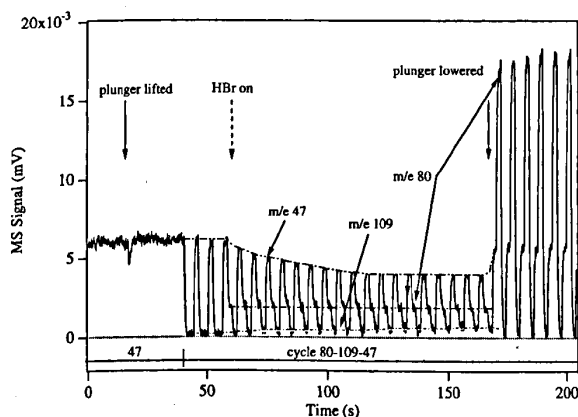


Fig. 4

Steady state experiment on the interaction of HBr ( $F = 3.45 \cdot 10^{15}$  mol/s) and HONO ( $F = 3.65 \cdot 10^{15}$  mol/s) on ice at 190 K in the 8 mm orifice reactor. The numbers at the bottom give the mass filter settings. At 20 s the plunger is lifted thus exposing HONO to the ice surface. Turning on the HBr flow at about 60 s results in the continuous uptake of HONO (upper trace) and the production of BrNO ( $m/e$  109, lower trace) with unitary yield. The middle trace represents the interaction of HBr ( $m/e$  80) with the ice surface

one observed on a pure ice surface (see above) and is not affected by the flow of HONO. After closing the sample support by lowering the plunger the HONO signal returned to its initial value whereas the BrNO signal vanished thus showing that the product formation is due to the interaction with the ice.

In a series of steady state experiments the reaction of HONO and HBr was studied under various initial HBr concentrations between 180 and 200 K. The experiments were conducted in different ways in order to obtain information on the role of HBr: i) the ice surface was exposed to a flow of HBr for several minutes and then exposed to a HONO flow, ii) after doping the ice surface with a given amount of HBr it was exposed to a concurrent flow of HBr and HONO, iii) the pure ice surface was exposed to a concurrent flow of HONO and HBr. In the first case (i) HONO was taken up initially with an uptake coefficient of up to  $2 \cdot 10^{-2}$ . After 1 min a steady state in the partial pressure of HONO was established corresponding to an uptake coefficient of approximately  $1 \cdot 10^{-3}$  which is a factor 20 lower than the initial value. From our data no significant dependence of the steady state uptake coefficient of HONO on the HBr dose or the HONO flow was found when the experimental protocol was carried out as under i) above. In the investigated temperature range of 180 to 210 K no temperature dependence of the initial and the steady state uptake coefficient of HONO was observed. Calculation of the amount of HBr incorporated into the ice and the amount of HONO taken up until the steady state is reached showed that only about 10 to 20% of the HBr in the condensed phase undergoes reaction with HONO. With a concurrent flow of HONO and HBr (see ii) and iii) above) the HONO

uptake remained constant and enhanced by a factor of up to 20 compared to the steady state uptake of HONO in the absence of a HBr flow but sufficient quantity of HBr in the condensed phase following protocol (i). As shown in Fig. 5 the uptake of HONO clearly depends on the given HBr concentration and tends to reach an upper limit which may be of the same order of magnitude as the uptake coefficient of HONO on frozen HBr solutions presented above. Turning off the HBr flow causes a decrease in the HONO uptake and a new steady state corresponding to  $\gamma = 1 \cdot 10^{-3}$  is obtained. Turning the HBr flow on again results in an increase of the uptake to its former value corresponding to the HBr flow (see Fig. 5). The reaction can be controlled by the HBr gas phase concentration. The absence of HBr in the gas phase results in a minimum uptake coefficient of  $1 \cdot 10^{-3}$ , whereas high HBr gas phase concentration results in a maximum uptake coefficient of up to  $2.2 \cdot 10^{-2}$ . The only difference between dosing the ice surface with HBr prior to reaction or not is the time it takes to establish the steady state (Fig. 6). On a dosed ice surface according to experiment (ii) the steady state is reached at once, whereas the HONO concentration takes between 1 and 2 min to attain steady state without dosing according to experiment (iii). Between 180 and 200 K the rate of reaching steady state shows no temperature dependence. However, for the concentration range of HBr used in this study the rate is slightly accelerated with increasing HBr concentration. As an illustration examples of the three series of experiments are shown in Fig. 6. In the range between 180 and 200 K a temperature dependence of the uptake coefficient of HONO at concurrent flow conditions could not be observed. Consideration of the mass balance obtained the result that HONO is quantitatively converted into BrNO whereas only about 50 to 70% of the HBr taken up reacted heterogeneously to BrNO (Fig. 7). The uptake of HBr in the presence of HONO remained

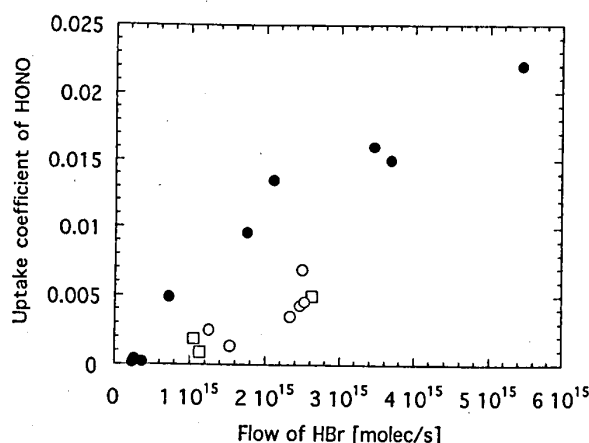


Fig. 5 Uptake coefficients of HONO at 190 K as a function of the HBr flow. All data were determined at a concurrent flow of HBr and HONO. The solid circles represent the uptake onto an ice surface, open circles onto solid H<sub>2</sub>SO<sub>4</sub> (concentrations from 10 to 60 wt% H<sub>2</sub>SO<sub>4</sub>) and the open squares onto a 1 M frozen KBr solution. Experimental conditions are given in Tables 5 and 6

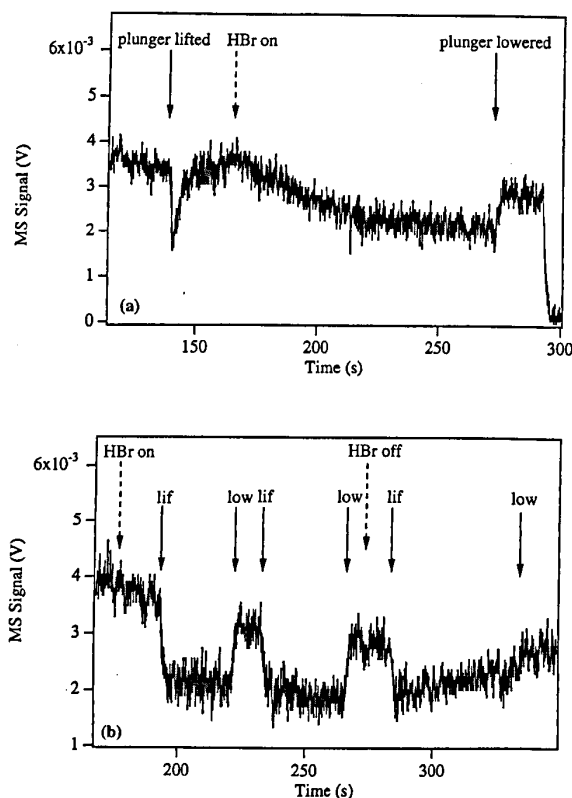


Fig. 6

MS traces showing the interaction of HONO with ice. The HONO signal is followed at  $m/e$  47. In Fig. 6a HONO ( $F = 3.11 \cdot 10^{15}$ ) is exposed to a pure ice surface. The plunger is lifted at 140 s resulting in an uptake of HONO followed by saturation. At 170 s the HBr flow ( $F = 2.2 \cdot 10^{15}$ ) is turned on and a decrease of HONO to a new steady state is observed. Fig. 6b shows an experiment where the ice surface was dosed with HBr prior to exposure to HONO ( $F = 2.80 \cdot 10^{15}$ ). The plunger operation is indicated by lif (plunger lifted) and low (plunger lowered). After turning on the HONO flow (not shown) and the HBr flow ( $F = 2.2 \cdot 10^{15}$ ) the plunger is lifted at 200 s resulting at once in a new steady state of HONO. Turning off the HBr flow at 280 s the HONO signal increases to a new steady state which corresponds to a lower uptake of HONO

unchanged compared to the uptake on a pure ice surface. Experimental results are summarized in Table 5.

All these observations point towards a complex adsorption process for HBr. The HBr taken up by the ice apparently exists in two different forms and only one component is reactive towards HONO. By dosing the ice surface with HBr only a fraction of the total HBr in the condensed phase is available for reaction. Once it is consumed in reaction 1 the uptake rate of HONO slows down (Fig. 6b). A concomitant flow of HBr provides a stationary concentration of the reactive species and the reaction will take place at the maximum rate. Moreover, the result that the maximum uptake rate of HONO is obtained at a concurrent flow of HONO and HBr indicates that the reaction may take place at the interface of the ice and the gas phase and not in the bulk. An interpretation will be presented in more detail in the next chapter.

Table 5  
Results for the concurrent flow experiments of HONO and HBr on ice

$T$ [K]	$F^i$ HBr <sup>a)</sup> [mol/s]	$F^i$ HONO <sup>a)</sup> [mol/s]	$F^R$ HBr <sup>b)</sup> [mol/s]	$F^R$ HONO <sup>b)</sup> [mol/s]	$F$ BrNO <sup>c)</sup> [mol/s]	$\gamma$ (HBr)	$\gamma$ (HONO)	Orifice <sup>d)</sup>
180	2.41(15)	3.10(15)	2.20(15)	7.47(14)			1.2(-2)	8
180	2.95(15)	1.50(15)	2.64(15)	6.12(14)			2.2(-2)	8
180	2.56(15)	3.06(15)	2.52(15)	1.59(15)			8.8(-3)	4
190	7.20(14)	2.59(15)	6.83(14)	3.34(14)			4.9(-3)	8
190	5.45(15)	4.45(15)	4.80(15)	3.25(15)			2.2(-2)	4
190	2.67(14)	7.39(15)	2.61(14)	3.25(14)			4.0(-4)	4
190	3.45(15)	3.82(15)	3.05(15)	1.27(15)	1.30(15)	0.27	1.6(-2)	8
190	3.68(15)	2.96(15)	3.16(15)	9.11(14)			1.5(-2)	8
190	2.10(15)	2.96(15)	1.91(15)	8.67(14)			1.3(-2)	8
190	1.75(15)	2.86(15)	1.57(15)	6.43(14)	5.74(14)	0.30	9.6(-3)	8
190	3.67(14)	4.13(15)	3.62(14)	1.00(14)	1.60(14)	0.41	2.0(-4)	4
190	2.45(14)	4.05(15)	2.40(14)	8.00(13)	1.45(14)	0.41	1.7(-4)	4
200	2.64(15)	3.02(15)	2.33(15)	6.94(14)			9.7(-3)	8
200	2.64(15)	3.88(15)	2.80(15)	1.78(15)			7.0(-3)	4
200	1.87(15)	3.69(15)	1.78(15)	6.00(14)		0.18	1.5(-3)	4
200	1.32(15)	3.86(15)	1.26(14)	4.30(15)		0.17	1.3(-3)	4
200	2.18(15)	3.19(15)	2.11(15)	1.38(15)			6.5(-3)	4
200	2.18(15)	2.77(15)	2.11(15)	1.48(15)			9.5(-3)	4
190 <sup>e)</sup>	1.13(15)	6.95(15)	1.09(15)	7.16(14)	8.87(14)	0.26	8.8(-4)	4
190 <sup>e)</sup>	1.05(15)	4.02(15)	9.77(14)	7.40(14)	8.54(14)	0.27	1.9(-3)	4
190 <sup>e)</sup>	2.62(15)	3.84(15)	2.54(15)	1.50(15)	1.72(15)	0.30	5.0(-3)	4

<sup>a)</sup> Flow into the cell

<sup>b)</sup> Flow to the surface defined by  $F^i - F^{\text{out}}$

<sup>c)</sup> Flow from the surface

<sup>d)</sup> Diameter of orifice in mm

<sup>e)</sup> 1 M frozen KBr solution

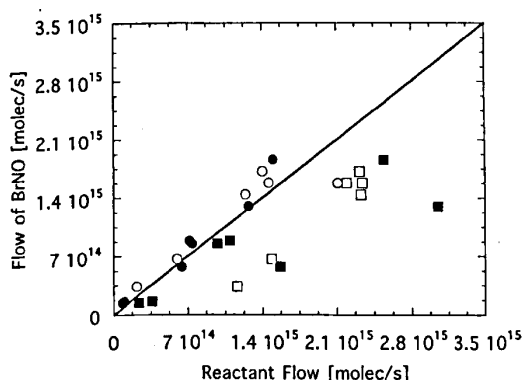


Fig. 7  
Flow of BrNO produced during the reaction of HONO and HBr on solid surfaces versus the reactant flows. Reactant flows are defined as  $F^i(\text{in}) - F^{\text{out}}$ . Circles represent the HONO flow: solid – ice, open – solid  $\text{H}_2\text{SO}_4$ , grey – 1 M frozen KBr solution. Squares represent the HBr flow: solid – ice, open – solid  $\text{H}_2\text{SO}_4$  (concentrations from 10 to 60 wt%  $\text{H}_2\text{SO}_4$ ), grey – 1 M frozen KBr solution. Experimental conditions are given in Tables 5 and 6

### 3.2.3 Reaction of HONO and HBr on Frozen KBr Solution

No BrNO could be observed by exposing a flow of HONO to a 1 M solution of KBr in water at 190 K. However, a concurrent flow of HBr and HONO in the presence of the surface resulted in formation of BrNO. The uptake of HONO is slightly lower than on a pure ice surface (Fig. 5) whereas the uptake of HBr is identical to the one on pure ice. Nevertheless, BrNO is produced in a yield of 100%

with respect to HONO. These data are included in Fig. 7 and Table 5.

### 3.2.4 Reaction of HONO and HBr on Solid $\text{H}_2\text{SO}_4$ Solutions

The reaction was studied at 190 K at  $\text{H}_2\text{SO}_4$  concentrations varying between 10, 40, 52, 60 and 95 wt%. The experiments have been performed in the same manner as the experiments on ice (see under 3.2.2) using a balancing water flow as described in the experimental section. In the presence of HONO the uptake behavior of HBr was identical to the one onto a  $\text{H}_2\text{SO}_4$  surface in the absence of HONO (Table 3) except at 95 wt%  $\text{H}_2\text{SO}_4$ , where an uptake coefficient of  $5 \cdot 10^{-4}$ , enhanced by a factor of at least 5 was observed (Fig. 8, Table 6). The uptake of HONO in the presence of a HBr flow corresponded to  $\gamma = 1 \cdot 10^{-3}$  to  $5 \cdot 10^{-3}$  over the whole  $\text{H}_2\text{SO}_4$  concentration range and had a slightly lower rate by approximately a factor of 2 compared to an ice surface. The observed dependence of the uptake of HONO on the given HBr flow is shown in Fig. 5. Determination of the yield of BrNO (included in Fig. 7) resulted in quantitative consumption of HONO under conditions of excess HBr in the condensed phase except for 95 wt%. At this  $\text{H}_2\text{SO}_4$  concentration only 10% of the HONO taken up reacts to BrNO. However, the yield of BrNO approaches  $100 \pm 25\%$  with respect to the small amount of HBr taken up indicating that the reaction of HONO and HBr is sensitive to the nature of the solid surface. The data are summarized in Table 6. The uptake of



Table 6

Experimental results for the uptake of HONO and HBr on frozen  $\text{H}_2\text{SO}_4$  solutions at 190 K

$\text{H}_2\text{SO}_4$ [wt%]	$F^i \text{HBr}^a)$ [mol/s]	$F^i \text{HONO}^a)$ [mol/s]	$F^R \text{HBr}^b)$ [mol/s]	$F^R \text{HONO}^b)$ [mol/s]	$F \text{BrNO}^c)$ [mol/s]	$\gamma (\text{HBr})$	$\gamma (\text{HONO})$	Orifice <sup>d)</sup>
10	1.53(15)	4.31(15)	1.49(15)	6.00(14)	6.66(14)	0.31	1.3(-3)	4
10	1.25(15)	3.05(15)	1.16(15)	2.18(14)	3.36(14)	0.42	2.5(-3)	8
40	2.46(15)	3.64(15)	2.33(15)	1.24(15)	1.44(15)	0.15	4.3(-3)	4
40	2.52(15)	3.92(15)	2.32(15)	1.40(15)	1.72(15)	0.1	4.6(-3)	4
52	2.33(15)	5.72(15)	2.18(15)	1.46(15)	1.58(15)	0.13	3.5(-3)	4
60	2.49(15)	4.64(15)	2.34(15)	2.11(15)	1.58(15)	0.13	6.9(-3)	4
95 <sup>e)</sup>	2.65(15)	2.80(15)	3.60(13)	1.60(15)	3.14(13)	1.1(-4)	6.1(-3)	4
95 <sup>e)</sup>	2.63(15)	3.96(15)	1.54(14)	1.29(15)	1.70(14)	5.2(-4)	4.0(-3)	4

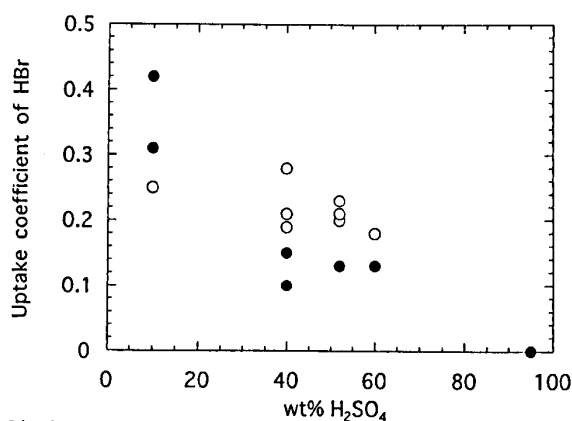
<sup>a)</sup> Flow into the cell<sup>b)</sup> Flow to the surface defined by  $F^{\text{in}} - F^{\text{out}}$ <sup>c)</sup> Flow from the surface<sup>d)</sup> Diameter of orifice in mm<sup>e)</sup>  $T = 220 \text{ K}$ 

Fig. 8

Uptake coefficient of HBr on frozen  $\text{H}_2\text{SO}_4$  solution as a function of the  $\text{H}_2\text{SO}_4$  concentration. Open circles represent the uptake of HBr onto  $\text{H}_2\text{SO}_4$  in the absence of HONO whereas the solid circles show the uptake of HBr in the presence of HONO. Experimental conditions are summarized in Tables 3 and 6

HONO on 10 and 40 wt%  $\text{H}_2\text{SO}_4$  in the absence of HBr was the same as that on a pure ice surface determined in Ref. [11] and control experiments in this work. At 52 and 60 wt% the amount of HONO taken up in the absence of HBr was below the detection limit of the mass spectrometer. At 95 wt%  $\text{H}_2\text{SO}_4$  an uptake of HONO of  $\gamma = 4 \cdot 10^{-3}$  was observed which is lower than the results obtained on liquid  $\text{H}_2\text{SO}_4$  solutions.

### 3.3 Reaction of HONO and HBr on Liquids

#### 3.3.1 Reaction of HONO and HBr on Liquid $\text{H}_2\text{SO}_4$

The reaction of HONO and HBr to BrNO according to reaction (1) proceeds also on liquid  $\text{H}_2\text{SO}_4$ . The reaction was studied on 40, 52, 60, 69, 80 and 95 wt% supercooled  $\text{H}_2\text{SO}_4$  at different temperatures (see Table 7) and at a balancing water flow. Most experiments were performed by exposing the sample to a concurrent flow of HBr and HONO. Over the whole concentration range of 40 to

95 wt%  $\text{H}_2\text{SO}_4$  both gases interact with sulfuric acid and BrNO is formed. However, the amount taken up strongly depends on the given  $\text{H}_2\text{SO}_4$  concentration unlike the results obtained on a frozen solution (Table 6). HBr shows greatest interaction at the lowest  $\text{H}_2\text{SO}_4$  concentration studied. In this case an uptake coefficient of  $4 \cdot 10^{-2}$  is obtained (Fig. 9) which is identical to the one without HONO. By increasing the  $\text{H}_2\text{SO}_4$  concentration the HBr uptake decreases to  $5 \cdot 10^{-4}$  at 95 wt% (Table 7). These findings are different from the results of HBr on sulfuric acid in the absence of HONO where no uptake was observed at high  $\text{H}_2\text{SO}_4$  concentrations (Table 3). This shows that the uptake of HBr may be enhanced by HONO in cases where only a low uptake rate for HBr is measured.

The interaction of HONO with sulfuric acid in the presence of HBr shows the opposite trend. At 95 wt%  $\text{H}_2\text{SO}_4$  the uptake of HONO attained the highest value with  $\gamma$  up to  $2.2 \cdot 10^{-2}$  which is not influenced by the presence of HBr. By lowering the  $\text{H}_2\text{SO}_4$  concentration the amount of HONO taken up decreases to a value of  $\gamma = 2 \cdot 10^{-3}$  at 69 wt% (Fig. 9). At a  $\text{H}_2\text{SO}_4$  concentration lower than 60 wt% in the presence of HBr the uptake of HONO remains constant at  $\gamma = 2 \cdot 10^{-3}$  in contrast to the observations in the absence of HBr where the uptake of HONO becomes immeasurably small [11]. At 40 wt% a slight increase in the uptake coefficient of HONO to  $5.5 \cdot 10^{-3}$  is observed in the presence of HBr. All determined uptake coefficients are summarized in Table 7. A few experiments have been performed by exposing the sulfuric acid first to one of the reactants with the higher uptake coefficient (HBr at lower  $\text{H}_2\text{SO}_4$  concentrations; HONO at the higher  $\text{H}_2\text{SO}_4$  concentrations) and subsequently to the second reactant. In these experiments the uptake of the second reactant HBr (or HONO) saturated after some time, however the initial uptake agreed with the value obtained using a concurrent flow.

The reaction product BrNO was observed over the whole  $\text{H}_2\text{SO}_4$  concentration range indicating that the uptake of HBr and HONO is reactive (Table 7) similar to the results on the frozen substrates. At low  $\text{H}_2\text{SO}_4$  concentrations

Table 7

Experimental results for the uptake of HONO and HBr on supercooled H<sub>2</sub>SO<sub>4</sub> solutions

H <sub>2</sub> SO <sub>4</sub> [wt%]	T [K]	F <sup>i</sup> HBr <sup>a)</sup> [mol/s]	F <sup>i</sup> HONO <sup>a)</sup> [mol/s]	F <sup>R</sup> HBr <sup>b)</sup> [mol/s]	F <sup>R</sup> HONO <sup>b)</sup> [mol/s]	F BrNO <sup>c)</sup> [mol/s]	γ (HBr)	γ (HONO)	Orifice <sup>d)</sup>
40	210	2.37(15)	4.04(15)	1.95(15)	7.80(14)	1.35(15)	3.9(-2)	4.2(-3)	4
40	210	1.96(15)	2.61(15)	9.12(14)	4.62(14)	2.04(14)	2.9(-2)	7.1(-3)	8
52	210	2.41(15)	5.42(15)	1.50(15)	8.11(14)	5.41(14)	1.7(-2)	1.9(-3)	4
52	210	2.30(15)	4.76(15)	1.79(15)	5.20(14)	3.99(14)	2.9(-2)	1.0(-3)	4
52	210	2.48(15)	5.56(15)	1.81(15)	1.41(15)	9.83(14)	2.2(-2)	2.8(-3)	4
60	220	2.72(15)	4.96(15)	7.25(14)	9.98(14)	4.20(14)	3.0(-3)	2.1(-3)	4
60	220	2.46(15)	4.47(15)	4.61(14)	8.40(14)	2.3(14)	1.9(-3)	1.9(-3)	4
60	220	2.14(15)	2.87(15)	1.51(14)	2.86(14)	4.5(13)	2.5(-3)	3.6(-3)	8
60	218	2.83(15)	4.15(15)	4.23(14)	5.91(14)	2.45(14)	1.5(-3)	1.9(-3)	4
60	218	2.56(15)	3.22(15)	1.06(14)	3.20(14)	1.17(14)	1.4(-3)	3.6(-3)	8
69	220	2.67(15)	5.55(15)	3.59(14)	7.09(14)	3.17(14)	1.3(-3)	1.5(-3)	4
69	220	2.17(15)	5.76(15)	2.6(14)	7.11(14)	2.30(14)	1.0(-3)	1.2(-3)	4
69	220	2.21(15)	1.01(16)	3.29(14)	1.22(15)	3.0(14)	1.5(-3)	1.1(-3)	4
69	230	2.46(15)	4.31(15)	2.40(14)	7.80(14)	2.13(14)	8.9(-4)	1.9(-3)	4
69	230	2.18(15)	3.94(15)	1.60(14)	4.35(14)	1.60(14)	2.6(-3)	4.1(-3)	8
80	258	2.68(15)	4.88(15)	1.42(14)	1.55(15)	8.43(13)	4.6(-4)	3.9(-3)	4
80	258	2.24(15)	3.47(15)	3.60(13)	1.86(14)		5.5(-4)	2.3(-3)	8
80	260	2.52(15)	6.06(15)	1.27(14)	2.58(15)	6.00(13)	4.3(-4)	6.1(-3)	4
80	260	2.18(15)	3.30(15)	8.31(13)	5.71(14)	5.10(13)	9.8(-4)	6.9(-3)	8
95	270	3.14(15)	2.79(15)	6.02(13)	1.08(15)	1.86(13)	6.4(-4)	2.2(-2)	8
95	270	1.98(15)	1.98(15)	1.04(14)	1.24(15)	9.00(13)	4.4(-4)	1.4(-2)	4

a) Flow into the cell

b) Flow to the surface defined by  $F^{\text{in}} - F^{\text{out}}$ 

c) Flow from the surface

d) Diameter of orifice in mm

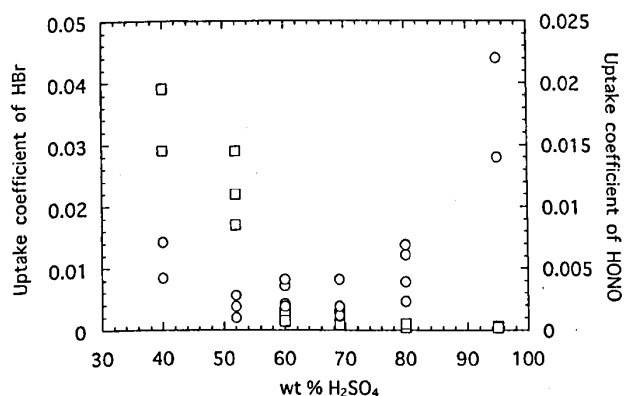


Fig. 9

Uptake coefficients of HONO and HBr onto liquid H<sub>2</sub>SO<sub>4</sub> as a function of the H<sub>2</sub>SO<sub>4</sub> concentration. Squares represent the uptake of HBr and circles the one for HONO. All uptake coefficients were determined using a concurrent flow of HBr and HONO. Experimental details are given in Table 7

characterized by a strong interaction of HBr and only a weak interaction of HONO the product yield is about 70% with respect to HONO taken up. In the opposite case, that is at high H<sub>2</sub>SO<sub>4</sub> concentrations such as 80 and 95 wt% H<sub>2</sub>SO<sub>4</sub> showing strong interaction with HONO and weak interaction of HBr, the yield of BrNO attains 100% with respect to HBr. However, at 70 wt% H<sub>2</sub>SO<sub>4</sub> a BrNO yield of 100% with respect to HBr and 50% with respect to HONO taken up is obtained. These results indicate that

BrNO is not as reactive on highly concentrated sulfuric acid solutions as the homologous ClNO [11].

The uptake of HONO onto sulfuric acid of various concentrations was studied in control experiments. Except for the 95 wt% H<sub>2</sub>SO<sub>4</sub> solutions the results were in good agreement with data reported in the literature [10, 11]. At high H<sub>2</sub>SO<sub>4</sub> concentrations the uptake coefficients were lower by a factor 2 to 5 and showed a large degree of scattering. As discussed earlier [11] this may be due to partial freezing of the H<sub>2</sub>SO<sub>4</sub> solution leading to hydrates with lower reactivity as shown in this work and reported in the literature [24, 25].

### 3.3.2 HONO on KBr/Methanol

In order to obtain information on the influence of the nature of the liquid a study of the interaction of HONO with a saturated solution of KBr in methanol at 190 K was performed. HONO was taken up by this liquid with an uptake coefficient of  $5 \cdot 10^{-2}$ . No product formation was observed. Exposing a sample of liquid methanol to a concurrent flow of HONO and HBr at 190 K led to an uptake of  $\gamma = 2 \cdot 10^{-2}$  for HONO and of  $\gamma = 0.1$  for HBr. No product formation was observed. If the sample chamber was isolated, the gas flows halted and the sample chamber subsequently reopened all adsorbed HONO desorbed back into the gas phase whereas no change in the MS signals at  $m/k = 80$  and 79 (HBr) was detected. These results indicate that HONO is taken up in a reversible manner on methanol and no reaction takes place between HONO and HBr.

#### 4. Discussion

In the previous chapter we presented experiments on the uptake of HBr and the heterogeneous reaction of HBr with HONO on a variety of different surfaces. On an ice surface the uptake of HBr was found to be large with  $\gamma = 0.32$  and not saturable. The large degree of scattering of the data presented in Fig. 2 was mainly due to a lower accuracy of the measurements at these high uptake rates. The determination of the uptake coefficient is based on the algebraic expression given in the experimental section which becomes increasingly inaccurate for small remaining signal strengths. It may also be possible that the scatter of the data is in part attributable to different ice morphology in different experiments. However, the sample preparation procedure was the same in all experiments and therefore the average number of crystal imperfections should be the same from one sample to the next.

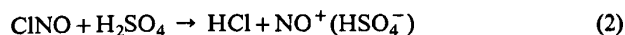
The determined uptake coefficient is in agreement with previous studies [14, 15, 18] where the physical uptake of HBr onto ice was determined to  $\gamma > 0.3$ . The authors concluded that the unlimited uptake is in analogy to the HCl/ice interaction [26] due to the formation of a HBr/H<sub>2</sub>O phase on the ice surface, perhaps in the form of hydrobromic acid trihydrate [18]. However, a recent study of the real time kinetics of the uptake of HBr onto ice [27] shows that in the temperature and concentration range used in this work no liquid layer is formed in contrast to the HCl system [28] indicating that the reaction between HBr and HONO does not occur in solution.

On liquid and solid H<sub>2</sub>SO<sub>4</sub> solutions the uptake of HBr depends on the H<sub>2</sub>SO<sub>4</sub> concentration. In addition, the solid H<sub>2</sub>SO<sub>4</sub> solutions are found to be more reactive towards HBr uptake by roughly a factor of 10. However, we are not able to exclude that patches of ice were formed on the solid H<sub>2</sub>SO<sub>4</sub> solutions so that the observed uptake rates represented the sum of a high uptake rate of HBr on ice and a small uptake rate on solid H<sub>2</sub>SO<sub>4</sub> solutions. No measurements of the uptake of HBr on solid H<sub>2</sub>SO<sub>4</sub> solutions have been reported in the literature. However, the uptake of HCl on sulfuric acid monohydrate [24] and sulfuric acid tetrahydrate [25] has been investigated. The authors found that the uptake of HCl strongly depended on the thermodynamic state of the substrate, that is the H<sub>2</sub>O partial pressure. In our experiments the partial pressure of water decreases from  $3 \cdot 10^{-4}$  Torr for 10 wt% H<sub>2</sub>SO<sub>4</sub> (which is close to the equilibrium vapor pressure of ice at 190 K) to about  $1 \cdot 10^{-5}$  Torr at 95 wt% H<sub>2</sub>SO<sub>4</sub>. At the same time the uptake of HBr decreases from  $\gamma = 0.25$  to  $\gamma < 1 \cdot 10^{-4}$ . Zhang et al. [24] reported a similar decrease of the HCl uptake of about two orders of magnitude in the same H<sub>2</sub>O vapor pressure range. Recently, the interaction of HBr with liquid sulfuric acid was studied [16, 17]. The results are in qualitative agreement with the results presented here. Both groups found a decreasing solubility of HBr with increasing H<sub>2</sub>SO<sub>4</sub> concentration between 60 and 72 wt% H<sub>2</sub>SO<sub>4</sub>. However, a direct comparison cannot be made because the authors only reported Henry coefficients.

If HONO is present together with HBr the uptake of both species was found to be reactive and the product BrNO was observed to be formed on all surfaces studied. Nevertheless, the yield of BrNO depends on the type of surface used. On a solid surface with a high uptake rate of HBr, that is a H<sub>2</sub>O-rich substrate, the amount of HONO taken up was strongly enhanced compared to the case where HBr was absent and BrNO was obtained at a yield of 100% with respect to HONO taken up and of 70% with respect to HBr, even with HONO in excess in the gas phase. Comparison of the heterogeneous reaction of HBr and HONO on ice with the one of HCl and HONO on ice [11] shows certain similarities. The uptake coefficients for HONO in the presence of HBr are of the same order of magnitude as the one for the HCl reaction reported by Fenter and Rossi. They also found a similar dependence of the uptake of HONO on the HCl concentration. One difference lies in the yield of ClNO which is 100% with respect to HONO and HCl in cases where HONO was in excess in the gas phase. If enough HONO is available HCl is completely converted to ClNO whereas only a fraction of the HBr is converted to BrNO. This may be an additional hint to a complex adsorption process for HBr different from HCl.

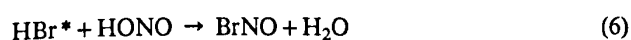
On liquid supercooled H<sub>2</sub>SO<sub>4</sub> solutions the uptake behavior of HONO and HBr seems to be more complex. The H<sub>2</sub>SO<sub>4</sub> concentration range studied in this work may be divided into three parts: a) the low concentration range (40, 50 wt%) characterized by high HBr uptake and low HONO interaction, b) the medium concentration range (60, 70 wt%) where both uptake coefficients are at a minimum value and c) concentrations higher than 70 wt% characterized by high HONO and low HBr uptake. Comparison of the uptake coefficients of HONO determined in the presence of HBr to the uptake of HONO in the absence of HBr [11, 29] indicates that the uptake is only enhanced by a factor of 10 in the range of 50 to 60 wt% H<sub>2</sub>SO<sub>4</sub> solutions. At higher H<sub>2</sub>SO<sub>4</sub> concentrations the uptake of HONO is large due to the formation of  $\text{NO}^+\text{HSO}_4^-$  as reported in the literature [10, 11, 29, 30]. At 40 wt% H<sub>2</sub>SO<sub>4</sub> a slight increase in the uptake coefficient of HONO was observed which is in qualitative agreement with the results of Becker et al. [29]. They found an exponential decrease in the effective Henry coefficient between 0 and 53 wt% H<sub>2</sub>SO<sub>4</sub> which is attributed to a salt effect. The uptake of HBr is enhanced by at least a factor of 5 in the presence of HONO at concentrations higher than 70 wt% H<sub>2</sub>SO<sub>4</sub> in contrast to the HCl/HONO system [11] where no reaction was observed at concentrations higher than 65 wt%. However, it is interesting to note that the formation of BrNO has been observed over the whole H<sub>2</sub>SO<sub>4</sub> concentration range at a nearly constant rate unlike the HCl/HONO system where ClNO formation was only observed between 55 and 65 wt% H<sub>2</sub>SO<sub>4</sub> [11]. As already pointed out, this may indicate a lower reactivity of BrNO on liquid H<sub>2</sub>SO<sub>4</sub> compared to the homologous ClNO. The difference of the systems HCl/HONO and HBr/HONO on liquid H<sub>2</sub>SO<sub>4</sub> could well be due to the different reactivity of the products. Fenter and Rossi [11] found that ClNO is

readily taken up by highly concentrated  $\text{H}_2\text{SO}_4$  solutions forming HCl according reaction 2:



If ClNO is formed in the reaction of HONO with HCl it reacts with  $\text{H}_2\text{SO}_4$  to HCl and in the case of a sufficiently high rate of reaction 2 no net uptake of HCl will be observed. By assuming a lower rate for the reaction of BrNO with  $\text{H}_2\text{SO}_4$  relative to the one of ClNO BrNO may be released into the gas phase and a net uptake of HBr will be observed. If HBr is quantitatively consumed according to reaction 1 the yield of BrNO is 100% with respect to HBr under conditions of excess HONO regardless of the rate of the possible reaction of BrNO with  $\text{H}_2\text{SO}_4$  to HBr.

From the experiments presented here some conclusion concerning the mechanism of HBr uptake and the reaction may be drawn. As described in the previous chapter the maximum rate of BrNO formation is obtained on solid surfaces with an uptake coefficient of HBr larger than 0.1. Moreover, a continuous HBr flow is needed to maintain a constant reaction rate although the concentration of HBr in the condensed phase is found to be always in excess relative to the HONO concentration in the condensed phase. These results imply a complex adsorption process of HBr. Based on our observations (Figs. 6 and 7) we suggest a reaction sequence which may describe the adsorption process in a straightforward albeit complex mechanism (reaction 3 to 6). The first step, the uptake of HBr onto the ice surface S (reaction 3), should be a simple and therefore fast adsorption which is in agreement with the results presented here. If the species  $\text{HBr}_{(\text{ads})}$  is taken to be the reactive species HONO should be taken up at the maximum rate regardless of the dosing of the ice surface with HBr prior to HONO exposure. However, the maximum rate of BrNO formation is only obtained after a certain time in cases where the ice surface is not dosed with HBr prior to reaction (Fig. 6a). Therefore  $\text{HBr}_{(\text{ads})}$  has to be converted into  $\text{HBr}^*$  (reaction 5), which represents the active reactant. Only approximately 50% of the HBr taken up is able to react to BrNO. This indicates that there is a second channel in which HBr is unreactive towards HONO (reaction 4). After halting the HBr flow the reaction between HONO and HBr proceeds further albeit at a lower rate (Fig. 6b). This may be explained by the rate limiting back reaction of the reservoir P yielding  $\text{HBr}^*$  (reaction 4 and 5).



In a steady state experiment at a concurrent flow of HBr and HONO the HONO concentration may be expressed as:

$$0 = \frac{F^{\text{in}}}{V} - k_{\text{esc}} [\text{HONO}] - k_6 [\text{HONO}] [\text{HBr}^*] \quad (I)$$

$V$  represents the volume of the Knudsen reactor (Table 1),  $F^{\text{in}}$  the flow of HONO into the reactor and  $k_{\text{esc}}$  the rate constant for effusive loss. Assuming steady state conditions for  $\text{HBr}_{(\text{ads})}$  and  $\text{HBr}^*$  yields expression (II):

$$[\text{HBr}^*] = \frac{k_3 k_5 [\text{HBr}_{(\text{g})}] + k_{-4} [\text{P}]}{k_4 k_5 + (k_4 k_{-5}) k_6 [\text{HONO}]} \quad (II)$$

Combining Eqs. (I) and (II) yields expression (III) for the reactive HONO flow:

$$\frac{F_{\text{HONO}}^{\text{R}}}{V} = k_6 [\text{HONO}] \cdot \frac{k_3 k_5 [\text{HBr}_{(\text{g})}] + k_{-4} [\text{P}]}{k_4 k_{-5} + k_6 [\text{HONO}] (k_4 + k_5)} \quad (III)$$

The back reaction  $-5$  is assumed to be slow in the presence of HONO and the term  $k_4 k_{-5}$  may be neglected yielding:

$$F_{\text{HONO}}^{\text{R}} = V \frac{k_3 k_5 [\text{HBr}_{(\text{g})}] + k_{-4} [\text{P}]}{k_4 + k_5} \quad (IV)$$

As shown in Fig. 10, which uses the data of Fig. 7, a plot of the reactive flow of HONO,  $F^{\text{R}}$  defined as  $F^{\text{in}} - F^{\text{out}}$  versus the reactive flow of HBr, that is  $F^{\text{R}} = k_3 [\text{HBr}_{(\text{g})}] V$  yielded a slope of 0.6. This indicates that  $k_4$  and  $k_5$  should be of the same order of magnitude and the term  $k_{-4} [\text{P}]$  is less important than the term including  $[\text{HBr}_{(\text{g})}]$  in the presence of HBr in the gas phase. Without a continuous flow of HBr (Fig. 6b)  $k_{-4}$  is rate limiting.

This model is simple and conceals the complexity of a heterogeneous reaction and should therefore only be considered as an approximation. Especially the dependence of the uptake coefficient of HONO (Fig. 5) on the HBr con-

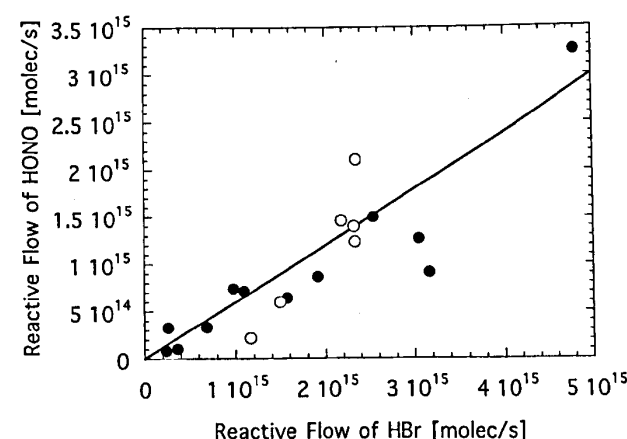
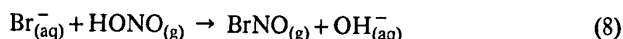


Fig. 10  
Reactive flow of HONO ( $F^{\text{in}} - F^{\text{out}}$ ) versus reactive flow of HBr. The solid line has a slope of 0.6 indicating that about 60% of the HBr taken up ends up reacting with HONO. The solid circles represent the experiments on an ice surface, open circles on solid  $\text{H}_2\text{SO}_4$  (concentrations from 10 to 60 wt%  $\text{H}_2\text{SO}_4$ ) and grey circles on 1 M KBr solution. Experimental details are given in Tables 5 and 6

centration points towards a more complex reaction mechanism. Although our data clearly show that not all HBr taken up is available for reaction, we only can speculate on the nature of P and HBr\*. FTIR studies of the interaction between HBr and ice show that HBr is dissociated [31]. Therefore it seems reasonable to assume that the equilibrium 7, - 7 lies to right side thereby favoring the ionic form of HBr.



As discussed already by Fenter and Rossi [11] HONO should react in molecular form. Apparently, the formation of nitrosyl sulfuric acid (NSA,  $\text{NO}^+\text{HSO}_4^-$ ) is not required for the reaction to occur. At the highest concentrated  $\text{H}_2\text{SO}_4$  where NSA formation is most favored the reaction of HBr and HONO shows the lowest rate (Table 7) in analogy to the system HCl/HONO. Therefore, the heterogeneous reaction between HONO and HBr probably proceeds via a nucleophilic substitution with the  $\text{Br}^-$  reacting as the nucleophile (reaction 8).



The results on highly concentrated liquid as well as on solid  $\text{H}_2\text{SO}_4$  solutions support this hypothesis. The dissociation of HBr to  $\text{H}_3\text{O}^+$  and  $\text{Br}^-$  is weak in these highly acidic media. Indeed, we have observed that the rate limiting step on the 80 and 95 wt%  $\text{H}_2\text{SO}_4$  for BrNO formation is the uptake of HBr and not of HONO as on the ice surface.

Furthermore our results indicate that water may play a critical role in the reaction of HONO and HBr. The decrease of the rate of reaction by using other surfaces than ice indicates that the reaction of HBr and HONO depends on factors which are not yet considered in the mechanism above. The dissociation of HBr into  $\text{H}_3\text{O}^+$  and  $\text{Br}^-$  takes place in all environments studied here, even though the actual ion concentration changes in the various solvents. However, this should not affect reaction 8 because  $\text{Br}^-$  and HBr are in equilibrium (reaction 7, - 7). A difference in the substrates under study is the number of free water molecules which are needed to dissociate HBr. It is reduced in all environments studied here relative to ice by a) replacing water molecules by other solutes like HBr,  $\text{H}_2\text{SO}_4$  or KBr and b) additional water molecules relative to ice are consumed to form hydrated ions. Moreover, BrNO is not formed in experiments where only  $\text{Br}^-$  is present. If the availability of protons is necessary for the BrNO formation to occur the reaction should proceed readily in the acid media. However, the rate of a nucleophilic substitution depends on two factors: the efficiency of the nucleophile and the stabilization of the leaving group. The first factor is given by the effective hydration of the HBr thus resulting in  $\text{Br}^-$  ions whereas the stabilization of  $\text{OH}^-$  requires protons in order to convert the unfavorable leaving group  $\text{OH}^-$  into the more favorable  $\text{H}_2\text{O}$ . Water as a solvent seems to be an ideal compromise between these two requirements.

The heterogeneous formation of the easily photolyzed BrNO may play a role in the partitioning of bromine species under certain atmospheric conditions. However, the HBr concentrations in the atmosphere are of the order of  $1 \cdot 10^7 \text{ mol/cm}^3$  [13] which is a few orders of magnitude lower than the densities used in this study; on the other hand, the atmospheric HONO concentration may reach levels up to  $2 \cdot 10^{11} \text{ mol/cm}^3$  [1-4] which is close to the concentrations we used in this study. We were able to show that the formation of BrNO is dependent on the HBr concentration and therefore it is questionable that the rate of BrNO formation is high enough to be significant under atmospheric conditions. Moreover, the uptake coefficient of HBr and the reaction of HBr with HONO on ice was determined for temperatures lower than common in the upper troposphere ( $T \approx 230 \text{ K}$ ). Between 180 and 200 K the uptake of HBr on ice shows a slight negative temperature dependence. Therefore, at tropospheric temperatures the uptake may even be lower and consequently the rate of reaction of HONO with HBr may also decrease. It is nevertheless possible that reaction 1 may be important in the presence of ice where there are no constraints on the HBr interaction. A more detailed modeling study is needed to assess if HBr accumulates on ice or sulfuric acid particles and to which extent BrNO may be formed.

The authors acknowledge the generous financial support of the Office Fédéral de l'Enseignement et de la Science (OFES) under projects 95.0551 (SALT) and 95.0549 (HALOTROP) performed in the framework of the EU program "Environment and Climate". We are grateful to Dr. Frederick Fenter and to Prof. Hubert van den Bergh for their support and interest.

## References

- [1] J.G. Calvert, G. Yarwood, and A.M. Dunker, *Res. Chem. Intermed.* **20**, 463 (1994).
- [2] U. Platt, D. Perner, G.W. Harris, A.M. Winer, and J.N. Pitts Jr., *Nature* **285**, 312 (1980).
- [3] D. Perner and U. Platt, *Geophys. Res. Lett.* **6**, 917 (1979).
- [4] R.M. Harrison and A.-M.N. Kitto, *Atmos. Environ.* **28**, 1089 (1994).
- [5] M.E. Jenkin, R.A. Cox, and D.J. Williams, *Atmos. Environ.* **22**, 487 (1988).
- [6] G.W. Harris, W.P.L. Carter, A.M. Wine, and J.N. Pitts, *Environ. Sci. Technol.* **16**, 414 (1982).
- [7] R.J. Salawitch, S.C. Wofsy, P.O. Wennberg, R.C. Cohen, J.G. Anderson, D.W. Fahey, R.S. Gao, E.R. Keim, E.L. Woodbridge, R.M. Stimpfle, J.P. Koplow, D.W. Kohn, C.R. Webster, R.D. May, L. Pfister, E.W. Gottlieb, H.A. Michelsen, G.K. Yue, M.J. Prather, J.C. Wilson, C.A. Brock, H.H. Jonsson, J.E. Dye, D. Baumgardner, M.H. Proffitt, M. Loewenstein, J.R. Podolske, J.W. Elkins, G.S. Dutton, E.J. Hints, A.E. Dessler, E.M. Weinstock, K.K. Kelly, K.A. Boering, B.C. Daube, K.R. Chan, and S.W. Bowen, *Geophys. Res. Lett.* **21**, 2251 (1994).
- [8] F. Arnold, J. Scheid, and Th. Stilp, *Geophys. Res. Lett.* **12**, 2421 (1992).
- [9] AERONOX, The Impact of  $\text{NO}_x$  Emissions from Aircraft Upon the Atmosphere at Flight Altitudes 8-15 km, ed. by U. Schumann, Final Report to the Commission of European Communities, 1995.
- [10] R. Zhang, M.-T. Leu, and L.F. Keyser, *J. Phys. Chem.* **100**, 339 (1996).

- [11] F.F. Fenter and M.J. Rossi, *J. Phys. Chem.* **100**, 13765 (1996).
- [12] B.J. Finlayson-Pitts, J.N. Pitts Jr., *Atmospheric Chemistry*, John Wiley & Sons, New York, 1986.
- [13] D.G. Johnson, W.A. Traub, K.V. Chance and K.W. Jucks, *Geophys. Res. Lett.* **22**, 1373 (1995).
- [14] D.R. Hanson and A.R. Ravishankara, *J. Phys. Chem.* **96**, 9441 (1992).
- [15] J.P.D. Abbatt, *Geophys. Res. Lett.* **21**, 665 (1994).
- [16] J.P.D. Abbatt, *J. Geophys. Res.* **100**, 14009 (1995).
- [17] L.R. Williams, D.M. Golden, and D.L. Huestis, *J. Geophys. Res.* **100**, 7329 (1995).
- [18] L.T. Chu and J.W. Heron, *Geophys. Res. Lett.* **22**, 3211 (1995).
- [19] F.F. Fenter, F. Caloz and M.J. Rossi, *J. Phys. Chem.* **98**, 9801 (1994).
- [20] F.F. Fenter, F. Caloz and M.J. Rossi, *J. Phys. Chem.* **100**, 1008 (1996).
- [21] F. Caloz, F.F. Fenter, K.D. Tabor, and M.J. Rossi, Design and Construction of a Knudsen-Cell Reactor for the Study of Heterogeneous Reactions over the Temperature Range 130–750 K, Performances and Limitations, subm. to *Rev. Sci. Instr.*, 1996.
- [22] Gmelins Handbuch der anorganischen Chemie, Brom Nr. 7, Verlag Chemie, Berlin, 1937.
- [23] G. Vuillard, *Compt. Rend.* **246**, 3252 (1958).
- [24] R. Zhang, M.-T. Leu, and L.F. Keyser, *J. Geophys. Res.* **100**, 18845 (1995).
- [25] R. Zhang, J.T. Jayne, and M.J. Molina, *J. Phys. Chem.* **98**, 867 (1994).
- [26] P.J. Wooldridge, R. Zhang, and M.J. Molina, *J. Geophys. Res.* **100**, 1389 (1995).
- [27] B. Flückiger and M.J. Rossi, unpublished results.
- [28] B. Flückiger, A. Thielmann, L. Gutzwiller, and M.J. Rossi, Real Time Kinetics of the Uptake of HCl on Water Ice in the Temperature Range 190 to 210 K, submitted to *Ber. Bunsenges. Phys. Chem.* (1997).
- [29] K.H. Becker, J. Kleffmann, R. Kurtenbach, and P. Wiesen, *J. Phys. Chem.* **100**, 14984 (1996).
- [30] J.D. Burley and H.S. Johnston, *Geophys. Res. Lett.* **19**, 1363 (1992).
- [31] H. Rieley, H.D. Aslin, and S. Haq, *J. Chem. Soc. Faraday Trans.* **91**, 2349 (1995).

(Received: November 4, 1996  
final version: March 14, 1997)

E 9421